Direct Geo-Rectification of Regional-Scale SAR Mosaics Using SRTM DEM Data

Yongwei Sheng
Department of Environmental Resources and Forest Engineering
State University of New York College of Environmental Science and Forestry
312 Bray Hall
1 Forestry Drive
Syracuse, NY 13210, USA
Email: ysheng@esf.edu

Keywords: ortho-rectification, SAR mosaics, topographic distortions, SRTM DEM.

ABSTRACT: SAR mosaics are often not precisely geo-referenced because topographic distortions were not removed during the mosaicking process due to the lack of adequate digital elevation models (DEMs). The Shuttle Radar Topography Mission (SRTM) has recently provided high-resolution DEM data with nearly global coverage, and makes it possible to geo-rectify SAR mosaics. Though techniques are available for rectifying individual scenes of SAR imagery using DEM data, these methods encounter difficulties when rectifying SAR mosaics because abrupt geometric discontinuities occur in SAR mosaics at scene boundaries. This paper introduces an automated direct method to directly removing geometric and topographic distortions and discontinuities from SAR mosaics and producing ortho-rectified mosaics, without accessing original SAR images. The proposed method was applied to geo-rectifying the Amazon basin GRFM (Global Rain Forest Mapping project) SAR mosaic produced from thousands of JERS-1 SAR images. Validation results show that 1-pixel (i.e., 92 m) positioning accuracy (root mean square error) was achieved in both the high Andes Mountains and the flat Atlantic estuaries, compared to the 16-pixel error (i.e., 1,380 m) of the original mosaics. The proposed procedures were implemented at a high level of automation with little human intervention. The large data volume represented by the Amazon basin mosaic is manageable on a PC computer. With the release of high-resolution SRTM DEM data, the proposed method is readily applicable to SAR mosaics located between 56^{o}S to 60^{o}N.

1 INTRODUCTION

Synthetic aperture radar (SAR) data are ideal for land surface mapping owing to their high spatial resolution and ability to penetrate clouds and darkness. Mosaics produced from SAR images serve as valuable base maps, especially in broad remote areas such as rain forest and boreal forest regions [1-7]. These data sets are extremely valuable for scientific research since in-situ observations are usually sparse and optical remote sensing technologies are often disabled due to cloud coverage. However, these SAR mosaics are usually not precisely geo-referenced because topographic distortions were not removed during the mosaicking process due to the lack of adequate digital elevation models (DEMs), thus their scientific value is severely limited. The SRTM (Shuttle Radar Topography Mission) mission has recently provided interferometrically-generated DEM data at a spatial resolution of 3 arc second (i.e., ~92 m around the Equator) with nearly global coverage (between 56^{o}S to 60^{o}N) [8]. This makes it possible to precisely geo-reference SAR mosaics and remove topographic distortions, thus produce ortho-rectified SAR mosaics.

SAR image rectification using DEM data is a mature technique, which has been in use for two decades [9-15]. However, this technique has been used exclusively to rectify individual scenes of SAR imagery. To produce precisely geo-referenced SAR mosaics, this technique would need to start over from the very beginning and repeat the entire mosaicking process, accessing individual original SAR scenes, removing topographic distortions, rectifying individual scenes, and mosaicking them. Re-processing such an enormous amount of data would require not only powerful computing facilities but also tremendous human power and efforts. This is prohibitive at the user level. A practical solution is to correct the geometric distortions in the SAR mosaics directly. Without accessing and reprocessing individual scenes of JERS-1 imagery, this paper contributes an automated method to rectifying geometric and topographic distortions in SAR mosaics using a localized rectification model with massive tie-points, and thus producing ortho-

rectified SAR mosaics.

The study area in this research covers the entire Amazon basin from 78°W to 48°W in longitude and 4°N to 16°S in latitude. The total area of the site is about 7.3 million km^2. This area comprises a diversified landscape, with the Atlantic estuaries in the east, the Amazon floodplains in the middle, and the high Andes Mountains in the west. The topography is dominated by the Andes Mountains in the western portion of the area with the extreme elevation of ~7680 m. Through the Global Rain Forest Mapping (GRFM) project, high-resolution regional-scale SAR mosaics were produced from thousands of JERS-1 L-band SAR images for the Amazon basin at a spatial resolution of 3 arc seconds for both low-water (October/November 1995) and high-water (May/June 1996) seasons [16]. This paper uses the high-water SAR mosaic as the case study.

2 THE SAR MOSAIC RECTIFICATION METHOD

Typical geometric problems in SAR mosaics are illustrated in Fig. 1 with a sample portion (1000×1500 pixels) of the GRFM mosaic. In addition to severe foreshortening and layover effects in mountainous areas, the SAR mosaic also contains shifting, double features, and break-lines around the scene edges. These discontinuities and variations between adjoining scenes can result in the mis-interpretation of terrain and surface characteristics. More importantly, the mosaic is not properly geometrically aligned with cartographic maps due to these errors. To effectively correct geometric distortions in SAR mosaics, it is important for the SAR mosaic rectification method to be able to identify the above problems in the mosaics and mitigate them in the ortho-rectified mosaics to be produced.

As illustrated in Fig. 2, we propose an automated localized method to rectifying SAR mosaics, which uses a great quantity of tie-points acquired through matching the SAR mosaic and the pseudo SAR image

Fig. 1. Typical geometric problems in SAR

(as simulated from SRTM DEM data). This method requires three types of inputs: the GRFM SAR mosaic, the SRTM DEM, and the typical JERS-1 imaging geometry parameters (i.e., sensor altitude H, look angle θ, and the orbital azimuth angle β). H, θ and β are used in SAR image simulation from the SRTM DEM, and β is also used in extracting features parallel to the satellite orbit from the GRFM mosaic. A dense and a sparse feature point sets are extracted from the SAR mosaic and are used in the subsequent image matching. Image matching is used for two purposes: 1) to screen out unreliable points, and 2) to establish correspondence and find the offsets between the reliable feature points and their corresponding points in the counterpart image. Image matching is implemented in two stages for computational efficiency. The first-stage image

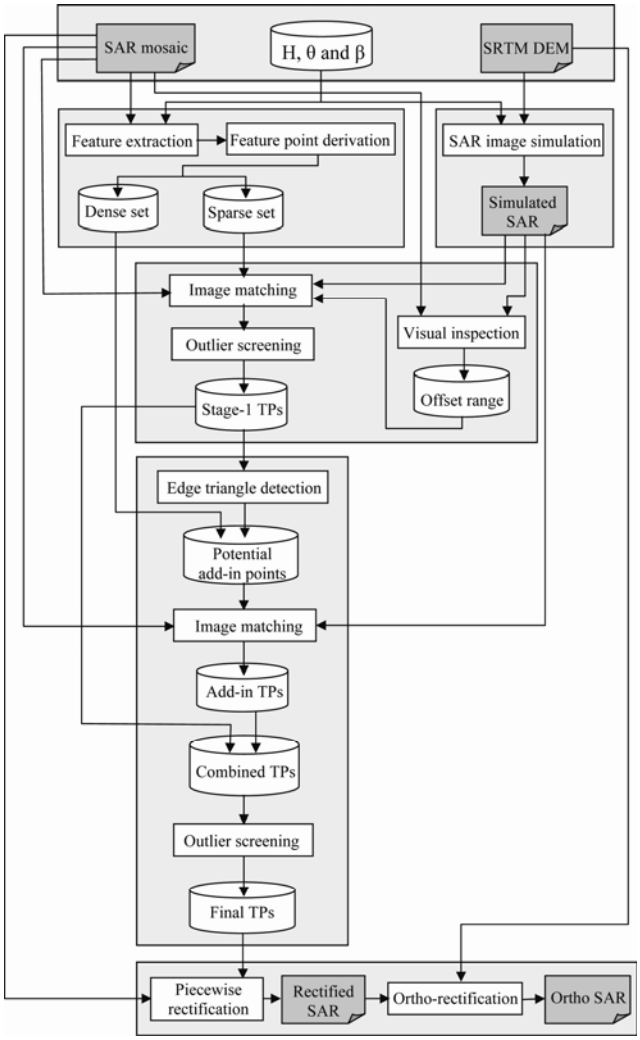

Fig. 2. Proposed SAR mosaic rectification scheme.

matching is implemented for the sparse point set only, and requires an input of the offset range between the GRFM mosaic and the simulated SAR image. The offset range is obtained through visual inspection of the two images, and this is the only manual action in the whole process. Those points passing the image matching and outlier screening are the tie-points derived from the first stage. Shifted scene edges may be located through triangulating these tie-points. Only those points in the dense feature point set around the detected scene edges participate in the second-stage image matching to better identify abrupt geometric changes. These stage-2 tie-points are then combined with the stage-1 tie-points for another outlier screening to produce the final set of tie-points for the rectification step. With the final set of tie-points, the SAR mosaic is then co-registered to the simulated SAR image using a localized rectification method rather than polynomial methods to ensure that abrupt geometric changes in the GRFM mosaic are corrected. The SAR mosaic is finally ortho-rectified by transforming the co-registered SAR mosaic back to the map coordinate system. The output of the above procedures is an ortho-rectified SAR mosaic with geometric and topographic distortions removed. Once the SAR mosaic is co-registered to the simulated SAR image, the ortho-rectification process is can be applied with the assistance of DEM data. The ortho-rectified SAR mosaic of the sample area (Fig. 1) is shown in Fig. 3, with both the foreshortening and layover effects removed.

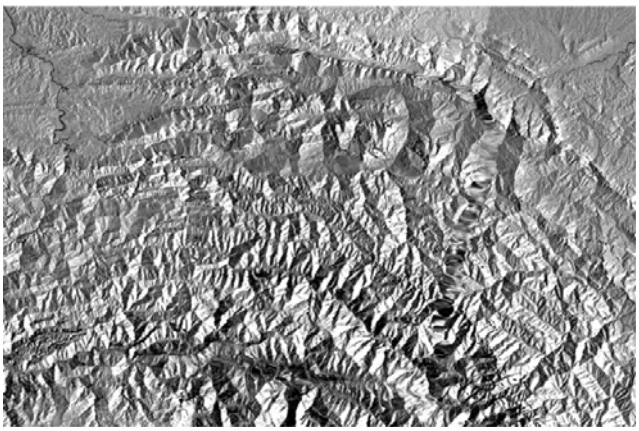

Fig. 3. Ortho-rectified SAR image.

3 SAR MOSAIC RECTIFICATION FOR THE ENTIRE AMAZON BASIN

The proposed procedures were implemented in IDL® (Interactive Data Language) on a Windows machine to geo-rectify the basin-wide GRFM mosaic. To ensure a complete coverage of the study area by properly ortho-rectified mosaics, the actual processed area is a half-degree lager around the border, making it a size of 21^o by 31^o and the mosaics in a size of 25,200×37,200 pixels. Due to the 1GB memory constraint of IDL on 32-bit Windows systems, it was not possible to feed the entire datasets into memory, instead the processed area was vertically divided into six sub-areas with one-degree overlap, and one piece was processed at a time.

The offset ranges between the GRFM mosaic and the simulated SAR image from DEMs were interactively determined to be [-32, +26] pixels (i.e., [-2,944, +2,392] m) in the X direction (i.e., West-East), and [-10, +15] pixels (i.e., [-920, +1,380] m) in the Y direction. With the proposed procedures, the GRFM mosaic was co-registered to the simulated SAR image by a piecewise rectification model using 984,085 automatically derived tie-points, and the ortho-rectified SAR mosaic was produced by transforming the co-registered SAR mosaic back the DEM coordinate system. The X and Y offset maps interpolated from these tie-points using TIN (triangulated irregular networks) models are shown in Fig. 4(a) and (b), respectively. About 60 individual scenes clearly stand out in the offset maps, with their offset values significantly different from those of their neighbors. These scenes are mostly located in high relief areas because of topographic distortions and ground control point (GCP) acquisition difficulties in these areas during the GRFM mosaicking process. The offsets are less significant in low elevation areas where topographic distortions in SAR imagery are minimal and where precise GCPs were relatively easy to select using well-defined drainage networks and river channels. In addition, the Y-direction offsets are less significant than the X-direction ones. This is not a coincidence but related to the sensor's characteristics. Due to the SAR imaging antenna geometry, the topographic distortions are mainly along the range direction. For the descending orbital JERS-1 SAR imagery that makes up the mosaics, the range direction is around 106^o from the North. Thus, the major topographic distortions are along the X direction, and result in larger offsets in the X direction than in the Y direction.

The whole proposed procedures were implemented at a high level of automation with little human intervention. The large data volume represented by the two Amazon GRFM mosaics was manageable on a PC machine (3.06 GHz processor). It took about 31 hours to process the mosaic, respectively. As expected, tie-point derivation through image matching was the most time-consuming process, taking

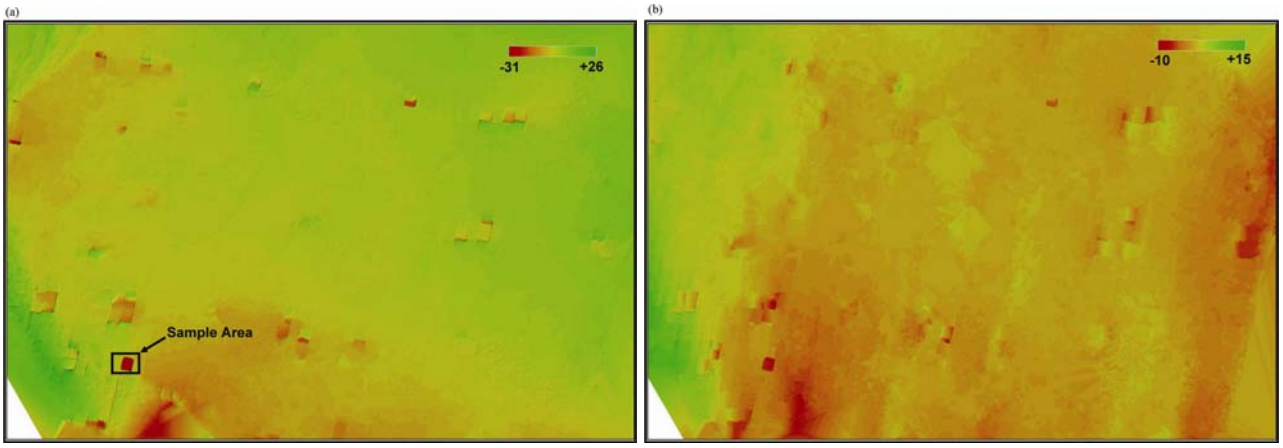

Fig. 4. Detected offset maps of high-water mosaic.

approximately 80% of the total CPU time. The two-stage implementation of image matching has already reduced the correlation expense significantly by 107%. Correlation computation may be further accelerated through FFT implementation [17]. In addition, the speed also depends on the quality of the original SAR mosaic. The process is expected to be faster for mosaics with a smaller offset range.

4 ACCURACY ASSESSMENT AND VALIDATION

The piecewise rectification technique is an exact deformation model passing through each tie-point and does not yield any geometric residuals, which would provide information about the correctness of rectification. Thus, independent checkpoint analysis is critical for determining the accuracy of piecewise rectification.

A systematic sampling scheme was taken in selecting checkpoints. A grid of 10×15 checkpoints was regularly laid out in this $20^{o}\times30^{o}$ study area with an even span of two degrees. Since the GRFM mosaic does not fully cover the study area, 144 checkpoints fall in the mosaic coverage. These checkpoints were finalized through visual inspection and manually shifted to the nearby salient feature points visible on both the original GRFM (or ortho-rectified) SAR mosaic and the SRTM DEM shading image. The positioning errors of the GRFM mosaic and the ortho-rectified mosaic are calculated for each checkpoint as the distance between its coordinates in the mosaic and in the shading image. For a quantitative error analysis, the mean error (MeanE), the maximum error (MaxE), and the root mean square error (RMSE) for 100m-interval altitudinal bands were computed from these checkpoints (Table 1). After ortho-rectification, the overall error measurements decrease significantly. The maximum error of the mosaic drops from 90.51 to 5.10 pixels, which implies that the positioning error is less than 5.10 pixels almost everywhere in the ortho-rectified mosaic. The mean error and the RMSE error drop from 8.67 to 0.60 pixels and 16.06 to 1.07 pixels, respectively. RMSE error is more statistically meaningful and commonly used in positioning error assessment. In terms of RMSE, the overall positioning accuracy of the ortho-rectified mosaic is about 1 pixel (i.e., 92 m), significantly smaller than the 16 pixels (i.e., 1,472 m) before rectification.

Altitude Range (m)	Checkpoint Counts	Mean Error		Maximum Error		RMSE	
		Before	After	Before	After	Before	After
0 - 99	31	3.53	0.91	11.05	5.10	4.80	1.51
100 - 199	40	4.63	0.78	12.17	4.47	5.57	1.23
200 - 299	35	6.79	0.49	24.75	1.42	8.40	0.79
300 - 399	13	5.75	0.19	14.57	1.41	7.06	0.48
400 - 499	5	5.80	0.57	12.37	1.41	6.99	0.89
500 and Up	20	30.63	0.22	90.51	1.41	39.89	0.50
Overall	**144**	**8.67**	**0.60**	**90.51**	**5.10**	**16.06**	**1.07**

Table 1. Accuracy assessment.

The error metrics exhibit spatial patterns. Fig. 13 shows the scatter plots of the positioning errors of the GRFM mosaic and the ortho-rectified mosaic against altitude. The errors of the GRFM mosaic are clearly related to topographic distortions, and increase exponentially to 90 pixels in higher altitudes (500 m and up). After ortho-rectification, the errors become independent of elevation, indicating that topographic

distortions have been successfully removed.

Table 1 lists the error metrics in 100 m altitudinal bands. Note the opposite trends of the metrics in the original GRFM mosaic and the ortho-rectified mosaic. In general, all error metrics of the GRFM mosaic increase with elevation, whereas they decrease with elevation after ortho-rectification. This is due to topographic distortions and owing to reliability of image matching. Since topographic distortions were not compensated during the GRFM mosaicking process, terrain relief induces larger positioning errors at higher elevations. On the contrary, topographic distortions have been removed from the ortho-rectified SAR mosaics, thus the positioning error should be independent of the elevation. Since the image matching is largely based on terrain feature points, denser and more reliable tie-points are usually found in high relief areas than low-altitude flat areas. The rectification accuracy is therefore better in high elevations. Even in the low-elevation bands, the error metrics become significantly smaller after the rectification. For example, the RMSE error in the 0-99 m band of the GRFM mosaic decreases from 4.80 to 1.51 pixels, respectively.

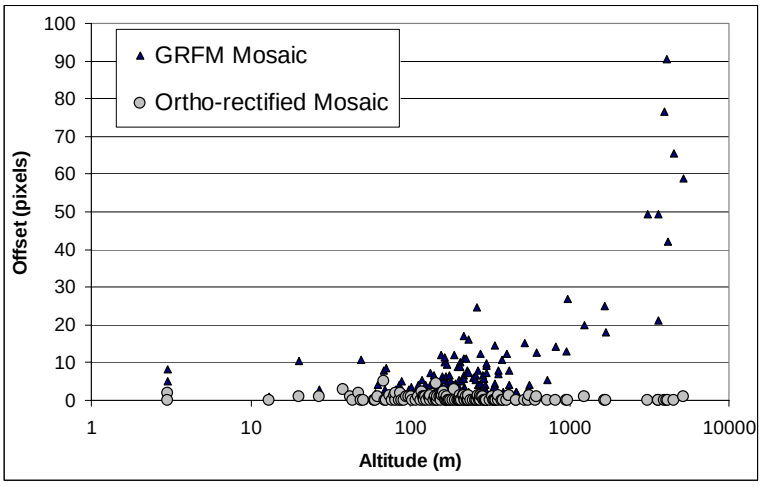

Fig. 5. Positioning error versus altitude.

Color composite images made from a SAR mosaic (as green channel) and the SRTM DEM shading image (as red channel) allow us to view the positional quality of the SAR mosaic. Three typical areas are selected for this compositing: a high relief mountainous area (Fig. 6; the sample area in Section 2), a low-elevation flat area (Fig. 7), and an area with great land cover variations (Fig. 8). Due to the severe topographic distortion in high relief areas, Fig. 6(a) shows great offsets (up to 80 pixels) between the GRFM mosaic and the DEM shading; while after the ortho-rectification (Fig. 6(b)), the positional properties of the ortho-rectified mosaic are improved significantly, matching the DEM layer with an accuracy better than 1 pixel. In low relief areas, SAR imagery less depends on topography. The lack of terrain features along the flat Atlantic coast may impose challenges to image matching, yet the proposed approach still effectively corrected the 10-pixel offsets in the original GRFM mosaic (Fig. 7). Though SAR backscatter variations due to land covers may affect image matching, the effective tie-point screening procedure developed to remove erroneous tie-points makes the proposed method relatively immune to the backscatter variations in SAR mosaics. Significant backscatter variations resulted from deforestation are shown in the color composite image (Fig. 8(a)), with forested areas (high backscatters) in green/yellow colors and deforested areas (low backscatters) in red. The ortho-rectified mosaic matches the DEM shading in Fig. 8(b), with the offsets between drainage features

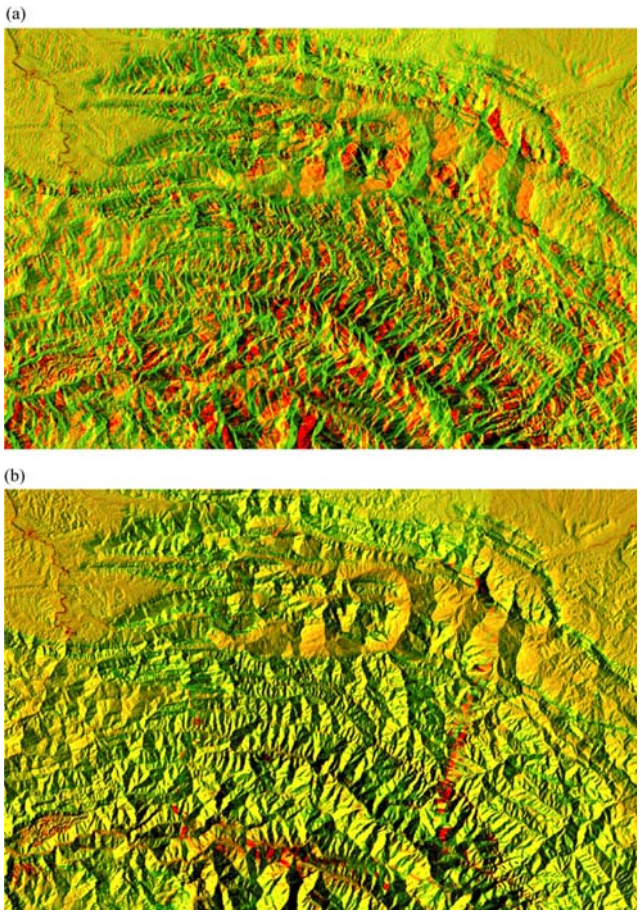

Fig. 6. Color composite images in high relief area.

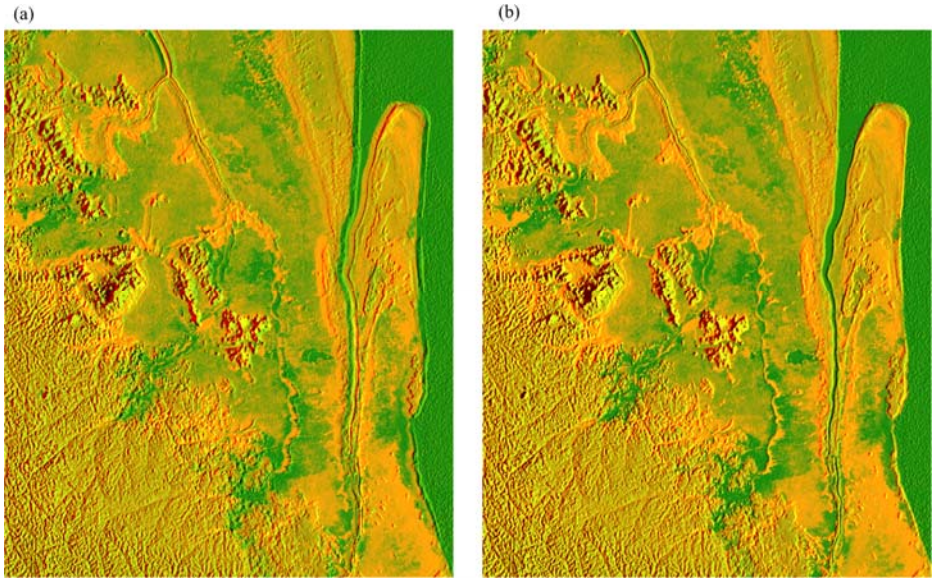

Fig. 7. Color composite images in flat area.

and terrain valleys (Fig. 8(a)) effectively removed. The green forest fragments stand higher than the surrounding red deforested areas.

From the above validation, it can be concluded that the geometric properties of the SAR mosaics are significantly improved using the proposed approach, with an overall accuracy of 1 pixel achieved. Once SAR mosaics have been geometrically rectified, a further step may be taken at the user level to correct radiometric distortions due to local incidence angle variations.

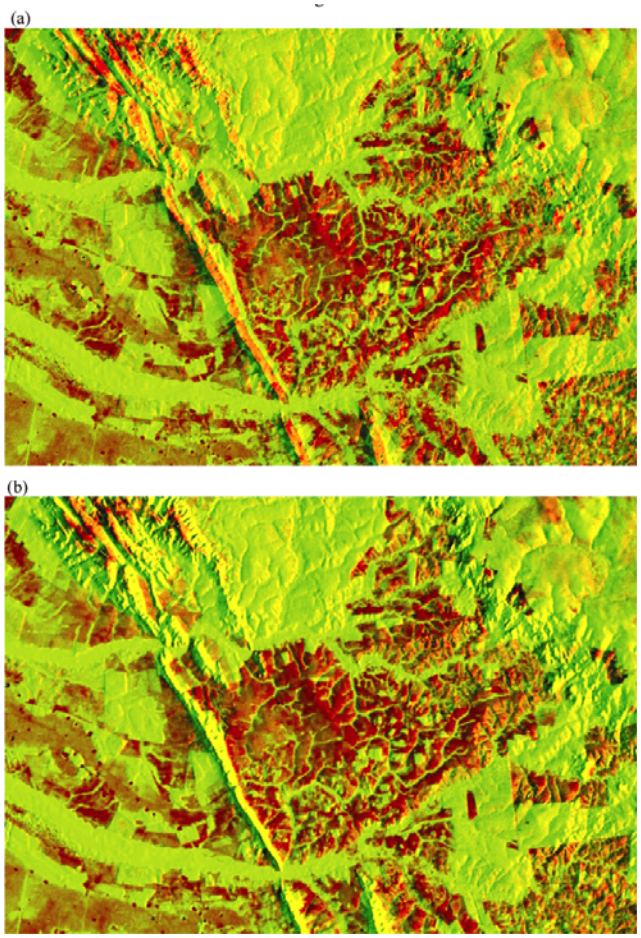

Fig. 8. Color composite images in an area with significant land cover variations.

5 CONCLUSIONS

This paper presents a direct method to geo-referencing and ortho-rectifying SAR mosaics without accessing the original scenes of SAR imagery. Critical techniques include two-stage implementation of image matching, outlier screening, and piecewise rectification. This method works largely because it allows rectification of abrupt geometric changes in SAR mosaics using a large number of reliable tie-points automatically derived through image matching. The two-stage image matching strategy significantly improves the computational efficiency, while the outlier screening and edge triangle detection procedures prevent backscatter variations and shifted scene edges from diminishing the quality of the rectified SAR mosaics. Since the piecewise deformation model is an exact-fit model, it is impossible to provide a correctness-of-fit measure (i.e., similar to such error measures typical of polynomial warping). Thus, it is critical for the outlier screening process to remove unreliable tie-points before rectification. The ortho-rectified SAR mosaics are largely free of geometric and topographic distortions (e.g., foreshortening and layover effects), and the overall positioning accuracy is achieved at about 1 pixel, both in mountainous and low elevation areas. This is sufficient for most scientific purposes. The method proposed in this paper is able to rectify any SAR mosaics wherever DEM data are available. With the release of global SRTM DEM data sets, the proposed method is readily applicable to any areas between 56^{o}S to 60^{o}N.

REFERENCES

[1] G. De Grandi, P. Mayaux, Y. Rauste, A. Rosenqvist, M. Simard, and S. S. Saatchi, "The Global rain forest mapping project JERS-1 radar mosaic of tropical Africa: development and product characterization aspects," *IEEE Transactions on Geoscience and Remote Sensing*, vol. 38, no. 5, pp. 2218-2233, Sept. 2000.

[2] A. K. Milne and Y. Dong, "Vegetation mapping using JERS-1 SAR mosaic for northern Australia," *International Journal of Remote Sensing*, vol. 23, no. 7, pp. 1475-1486 Apr. 2002.

[3] M. Shimada and O. Isoguchi, "JERS-1 SAR mosaics of Southeast Asia using calibrated path images," *International Journal of Remote Sensing*, vol. 23, no. 7, pp. 1507-1526, Apr. 2002.

[4] B. Chapman, P. Siqueira, and A. Freeman, "The JERS Amazon multi-season mapping study (JAMMS): observation strategies and data characteristics," *International Journal of Remote Sensing*, vol. 23, no. 7, pp. 1427-1446, Apr. 2002.

[5] P. Siqueira, S. Hensley, S. Shaffer, L. Hess, G. McGarragh, B. Chapman, J. Holt, and A. Freeman, "A continental scale mosaic of the Amazon basin using JERS-1 SAR," *IEEE Transactions on Geoscience and Remote Sensing*, vol. 38, no. 6, pp. 2638-2644, Nov. 2000.

[6] P. Siqueira, B. Chapman, and G. McGarragh, "The coregistration, calibration, and interpretation of multiseason JERS-1 SAR data over South America," Remote Sensing of Environment, vol. 87, no. 4, pp. 389-403, Nov. 2003.

[7] C.L. Williams, K. McDonald, and B. Chapman, "Global boreal forest mapping with JERS-1: North America," in *Proceedings of IGARSS'99*, Hamburg, Germany, 1999, Vol. 2, pp. 785-787.

[8] B. Rabus, M. Eineder, A. Roth, and R. Bamler, "The shuttle radar topography mission – a new class of digital elevation models acquired by spaceborne radar," *ISPRS Journal Photogrammetry & Remote Sensing*, vol. 57, no. 4, pp. 241-262, Feb. 2003.

[9] G. Domik, "Radar image simulation as a tool to analyze topographic effects on geometry and radiometry of radar imagery," in *Proceedings of the 1985 Machine Processing of Remotely Sensed Data Symposium*, Purdue University, 1985, pp. 248-253.

[10] J. C. Curlander, "Utilization of spaceborne SAR data for mapping," *IEEE Transactions on Geoscience and Remote Sensing*, vol. GE-22, no. 2, pp. 106-112, Mar. 1984.

[11] B. Guindon and H. Maruyama, "Automated matching of real and simulated SAR imagery as a tool for round control point acquisition," Canadian Journal of Remote Sensing, vol. 12, no. 2, pp. 149-158, June 1986.

[12] G. Domik and F. Leberl, "Multiple incidence angle SIR-B experiment over Argentina: generation of secondary image products," *IEEE Transactions on Geoscience and Remote Sensing*, vol. GE-24, no. 4, pp. 492-497, July 1986.

[13] R. Kwok, J. C. Curlander, and S. S. Pang, "Rectification of terrain induced distortions in radar imagery," *Photogrammetric Engineering & Remote Sensing*, vol. 53, no. 5, pp. 507-513, May 1987.

[14] F. W. Leberl, *Radargrammetric Image Processing*, Norwood, MA: Artech House, 1990.

[15] W. Linder and H.-F. Meuser, "Automatic Tiepointing in SAR images," in *SAR Geocoding: Data and Systems*, G. Schreier, Ed. Karlsruhe: Wichmann,1993, pp. 206-212.

[16] Tropical Rain Forest Information Center, "GRFM-South America Data Products," [Online]. Available: http://trfic.jpl.nasa.gov/GRFM/jersframe.html, last accessed: May, 2004.

[17] H. Xie, N. Hicks, G. R. Keller, H. Huang, and V. Kreinovich, "An IDL/ENVI implementation of the FFT-based algorithm for automatic image registration," *Computers & Geosciences* , vol. 29, no. 8, pp. 1045-1055, Oct. 2003.